Metallurgy and materials
Metalurgia e materiais

Reduction of electric arc furnace dust pellets by mixture containing hydrogen

http://dx.doi.org/10.1590/0370-44672017720174

Eduardo Junca[1]
http://orcid.org/0000-0002-7068-2583
Felipe Fardin Grillo[2]
Joner Oliveira Alves[3]
José Roberto Oliveira[2,6]
Thomaz Augusto Gisard Restivo[4]
Denise Crocce Romano Espinosa[5,7]
Jorge Alberto Soares Tenório[5,8]

[1]Universidade do Extremo-Sul Catarinense - UNESC, Programa de Pós-Graduação em Ciência e Engenharia de Materiais, Criciúma - Santa Catarina - Brasil.
eduardojunca@unesc.net

[2]Instituto Federal do Espírito Santo - IFES, Departamento de Engenharia Metalúrgica, Vitória - Espírito Santo – Brasil.
felipefarding@gmail.com

[3]Diretor do Instituto SENAI de Inovação em Tecnologias Minerais, Belém – Pará – Brasil.
joner.alves@cni.org.br

[4]Universidade de Sorocaba - UNISO, Departamento de Engenharia de Materiais, Sorocaba - São Paulo - Brasil.
thomaz.restivo@usp.br

[5]Universidade de São Paulo - USP, Departamento de Engenharia Química, São Paulo - São Paulo - Brasil.

E-mails.: [6]jroberto@ifes.edu.br, [7]espinosa@usp.br, [8]jtenorio@usp.br

Abstract

The large amount of dust generated in electric arc furnace aligned with its chemical composition makes this dust a potential source of iron in the direct reduction iron process. Thus, the aim of this research is to investigate the reduction of pellets produced with electric arc furnace dust using hydrogen as the reducing agent. The kinetic investigation was examined applying the differential method. In addition, the influence of reducing gas stream and temperature in the reduction process were investigated applying the Forced Stepwise Isothermal Analysis technique. The temperature studied varied from 500 to 1000°C with isothermals in each 50°C. The reducing gas was a mixture of 10% of hydrogen and 90% of argon. Then, the product characterization was carried out via scanning electron microscope and X-ray analysis. A thermogravimetric test showed a mass loss of 42 wt% due to the reduction of iron and zinc oxides. Besides this, the reduction occurred in three steps: 550-650°C, 700-800°C, 850-950°C. Between 550-650°C, the reduction was controlled by a nucleation mechanism with an Ea of 41.1 kJ/mol. In the second step (700-800°C), a mixed control between nucleation and diffusion was obtained with an Ea of 89.1 kJ/mol. Furthermore, a crust of iron was formed around the pellet, which hindered the reducing gas diffusion into the pellet. In the third stage (850-950°C), the formation of a sintered structure was noted, which decreased pore volume. The internal diffusion of reducing gases was determined as the controlling mechanism, with an Ea of 130.9 kJ/mol.

Keywords: electric arc furnace dust; hydrogen reduction; kinetic investigation; solid-gas reaction.

1. Introduction

The use of coal in the steel mills is a serious problem, since one of its by-products is carbon dioxide. This gas is one of the many existing gases responsible for greenhouse effects. In addition, the steel mills also generate several types of waste, such as sludge, dust, slag and gases. The electric arc furnace dust (EAFD) is one of these wastes, presenting several components, such as iron, zinc, calcium and lead (Nezhad and Zabett, 2016).

Researches have shown that the electric arc furnace dust (EAFD) is composed mainly of iron and zinc, in which these elements are present as oxides (Fe_2O_3, Fe_3O_4, FeO and ZnO) and/or zinc ferrite (Fe_2O_3.ZnO) (Ledesma *et al*., 2017; Sayadi and Hesami, 2017). These components make the EAFD an interesting material to be used in the direct reduction process. However, some investigations should be performed to apply this method. One important investigation is for the kinetic parameters, such as activation energy (Ea) and the controller mechanism.

The kinetic investigation can be performed applying the differential or the integral method (Khawam and Flanagan, 2006; Lin *et al*., 1999). However, the differential method is said to be more accurate to determine the controller mechanisms (Brown, 1998). The differential method is described according to Equation 1:

$$\frac{d\alpha}{dt} = k \cdot f(\alpha) \quad (1)$$

Where $\propto$ is the reacted fraction, t is the time, and k obeys the Arrhenius law (Equation 2) and $f(\alpha)$ are functions used in kinetic models for a gas-solid reaction.

$$k = A \exp\left(-\frac{Ea}{RT}\right) \quad (2)$$

Where, A is the pre-exponential factor, T is the absolute temperature (K), Ea is the activation energy and R is the universal gas constant.

The reduction of oxides by gaseous agents are mentioned as being a solid-gas reaction. Several controller mechanisms are mentioned and some equations are deducted, as can be seems in Table 1 (Chen *et al.,* 1998; Maqueda *et al*., 1996).

Mechanism	Symbol	f(α)
Phase boundary controlled	R2	$(1-\propto)^{1/2}$
Phase boundary controlled	R3	$(1-\propto)^{1/3}$
One-dimensional diffusion	D1	$1/\propto$
Two-dimensional diffusion	D2	$1/(-\ln(1-\propto))$
Three-dimensional diffusion (Jander)	D3	$(1-\propto)^{2/3}/(1-(1-\propto)^{1/3})$
Three- dimensional diffusion (Ginstling-Brounshtein)	D4	$1/([(1-\propto)^{-1/3}-1])$
Two-dimensional nucleation	A2	$(1-\propto)[-\ln(1-\propto)]^{1/2}$
Three-dimensional nucleation	A3	$(1-\propto)[-\ln(1-\propto)]^{2/3}$

Table 1
Mathematical suggestions for kinetic modeling for heterogeneous reactions of the gas-solid.

Thus, the aim of this research was to investigate the reduction of electric arc furnace dust using hydrogen as the gaseous agent and determine the kinetic parameters involved in this practice, since the use of hydrogen does not generate greenhouse gases and it is thermodynamically more favorable at higher temperatures.

2. Experiment

2.1 EAFD characterization

The EAFD characterization has been published previously (Junca *et al*., 2012; Junca *et al*., 2016). Thus, a summary will be mentioned. Table 2 shows the chemical composition of the electric arc furnace dust and the Table 3 shows the result of the Rietveld method for phase quantification. The main element in the EAFD is Fe (44.6 wt%) as magnetite (43.2 wt%), franklinite (21.6 wt%) and metallic iron (0.5 wt%). The zinc content is 15.9 wt% as zincite (28.8 wt%) and franklinite. Other elements, such as Ca, Si, Mn, Mg and Pb were also found. In addition, a size analysis showed that the EAFD is in the range of 0.158-158.489 µm, with 90% lesser than 50.89 µm and 50% lesser than 8.658 µm.

Elements	Fe_{total}	Fe0	Zn	Ca	Si	Mn	Mg	Pb
Percentage (%)	44.6	0.6	15.9	5.7	4.0	2.0	1.5	1.2

Table 2
Chemical composition of electric arc furnace dust.

Phases	Iron	Zincite	Quartz	Magnetite	Franklinite
Percentage (%)	0.5	28.5	6.2	43.2	21.6

Table 3
Phases quantification of the electric arc furnace dust determined via Rietveld method.

2.2 Pellet production

The pellets of EAFD were performed by a disc pellet adapted in a concrete mixer. Then, the pellets were conducted for the drying step. This step was carried out in two phases. The first, the pellets were dried at 200°C by 12 hours. The second phase, the pellets were heated at 700°C by 24 hours.

2.3 Thermogravimetric analysis

A pellet of EAFD was put into a Setsys Evolution Setaram thermobalance. The reducing gas flows were 50, 100, 150 and 200 mL/minute in order to investigate the transfer of the reducing gas to the pellet surface and core. The temperature influence on the reduction process was studied applying the FSIA method. Thus, the temperatures investigated were between 500-1100°C, with isotherms at each 50 °C. Each isothermal was kept for 15 minutes. A gaseous mixture containing 10 wt% of hydrogen and 90 wt% of argon was used.

2.4 Kinetic investigation

The control mechanisms and activation energy were obtained via a differential method. To it, the linear trends from the relationship $d(\alpha)/dt \times f(\alpha)$ were compared for all functions mentioned in Table 1, since the greater linear trend suggests the control function. The reacted fraction was calculated via Equation 3.

$$\alpha = \frac{m_0 - m_T}{m_0 - m_f} \quad (3)$$

Where, α is the reacted fraction; m_0 is the sample initial mass; m_T is the sample mass at temperature T and mf is the sample final mass.

Then, the Arrhenius curves ($\ln k \times 1/T$) were sketched out in order to calculate the Ea. In addition, the equations that did not present a linearity in the Arrhenius curves were not considered as a controlling mechanism, since the reaction rate was similar inside each step. Furthermore, increasing the temperature did not increase the reaction rate in the same step.

2.5 Product characterization

The product characterization was carried out using a Philips scanning electron microscope (SEM), XL-30 model. The pellets were taken off the thermobalance when the temperature reached 700 and 900 °C. This step was performed in order to investigate the morphological change at each temperature. In addition, X-ray analysis was performed after the complete reduction in order to identify the phases. A Rigaku diffractometer, Miniflex 300 model, equipped with Cu Kα (λ= 1,5418Å) tube was used.

3. Results and discussion

3.1 Thermogravimetric analysis

Figure 1a shows that increasing the gas flow also increases the reaction rate. A mass loss of 42 wt% for 200 mL/minute of gas stream was also noted. This value is from oxides (Fe_3O_4 and ZnO) and zinc ferrite (Fe_2O_3.ZnO) reduction. In addition, the reaction rate for gas streams of 100, 150 and 200 mL/ minute did not present a significant change on the reaction rate, which indicates that the transfer of the reducing gas to the pellet surface did not have influence on the reaction. On the other side, when the temperature was increased, the reaction rate changed (Figure 1b). Furthermore, it was noted that between some consecutive isothermals (650-700°C and 800-850°C), the reaction rate was altered, which indicates a change of control mechanism between these temperatures. Thus, the reduction of EAFD by hydrogen occurred in three steps: 550-650°C, 700-800°C and 850-950°C.

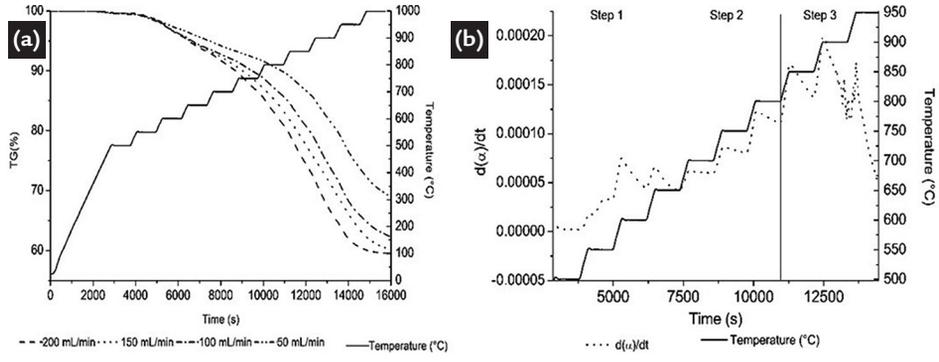

Figure 1
Thermogravimetric tests.
a) Influence of gas stream on the reduction of electric arc furnace dust pellet. b) Effect of the temperature on reduction reaction.

3.2 Kinetic investigation

At 500-650°C (Table 4), all functions presented a similar correlation factor. On the other hand, Table 5 shows that between 700-800°C the correlation factor for the functions A3, D1, D2, D3, D4, R2 and R3 were greater, which suggests that these functions presented a linear trend, and, therefore, they can be the controlling mechanisms. In the third step, for a temperature range of 850-950°C, the functions A2, D1, D2, D3, D4, R2 and R3 presented a greater correlation factor, as can be seen in Table 6. In a previous article (Junca *et al.*, 2016), the influence of the pellet diameter during a reduction

process with a similar reducing gas was investigated. It was concluded that up to 700°C the reaction rate was not affected for pellets with different diameters. This fact suggests that diffusion is not present in the range of 550-650°C.

Temperature (°C)	Control mechanism							
	A2	A3	D1	D2	D3	D4	R2	R3
550	0.66	0.65	0.74	0.74	0.69	0.62	0.62	0.62
600	0.78	0.79	0.70	0.70	0.67	0.80	0.80	0.80
650	0.99	0.98	0.99	0.99	0.98	0.98	0.98	0.98

Table 4
Correlation factor for the relationship $d(\alpha)/dt \times f(\alpha)$ for the temperature in the range of 550-650°C.

Temperature (°C)	Control mechanism							
	A2	A3	D1	D2	D3	D4	R2	R3
700	0.95	0.94	0.95	0.95	0.95	0.93	0.93	0.93
750	0.97	0.96	0.97	0.97	0.97	0.95	0.95	0.95
800	0.53	0.97	0.97	0.97	0.97	0.97	0.97	0.97

Table 5
Correlation factor for the relationship $d(\alpha)/dt \times f(\alpha)$ for the temperature in the range of 700-800°C.

Temperature (°C)	Control mechanism							
	A2	A3	D1	D2	D3	D4	R2	R3
850	0.94	0.73	0.98	0.98	0.98	0.97	0.97	0.97
900	0.98	0.97	0.99	0.99	0.99	0.99	0.98	0.99
950	0.99	0.99	0.99	0.99	0.99	0.99	0.99	0.99

Table 6
Correlation factor for the relationship $d(\alpha)/dt \times f(\alpha)$ for the temperature in the range of 850-950°C.

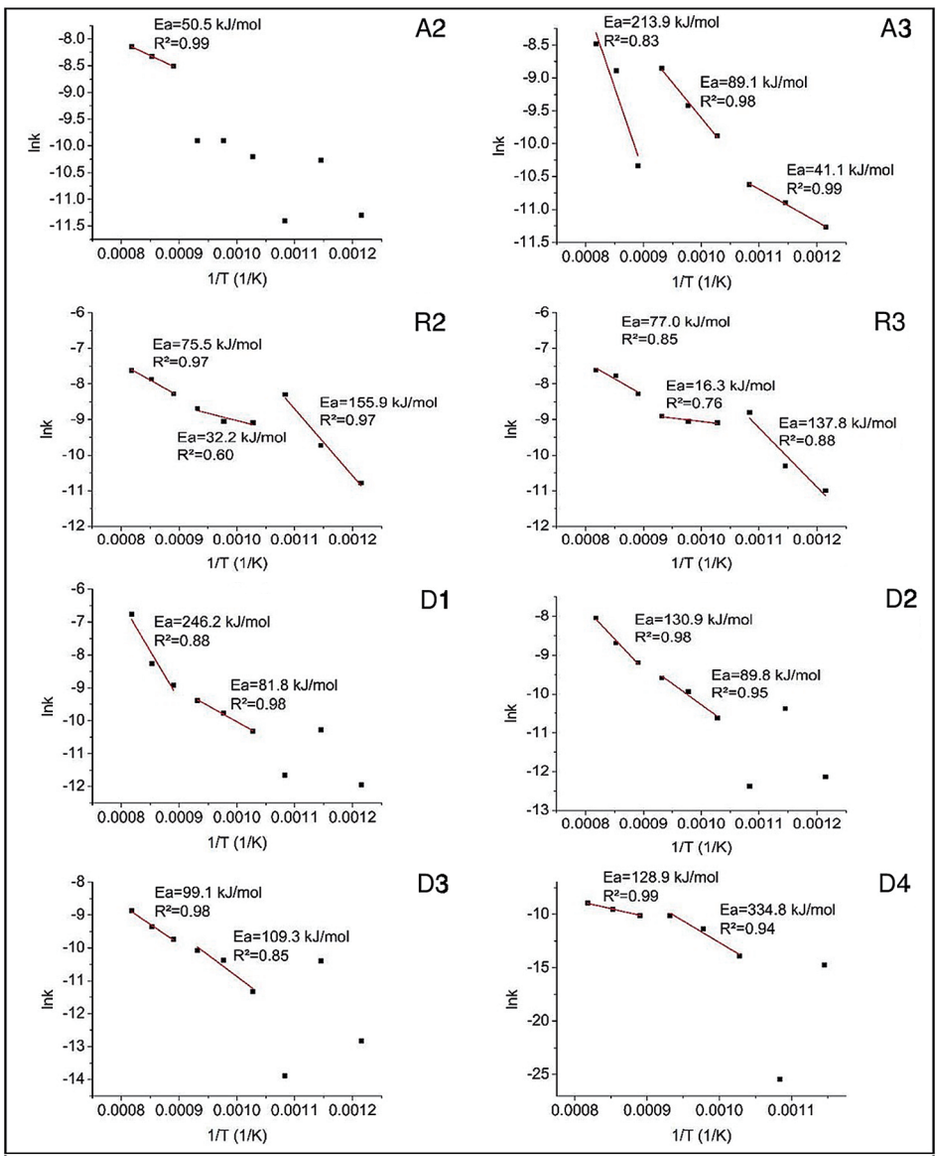

Figure 2
Arrhenius curve obtained to A2, A3, D1, D2, D3, D4, R2 and R3 functions.

For a temperature higher than 700°C, there was some influence on the reaction rate, which indicates that diffusion plays some influence above that temperature. According to Pineau *et al.*, (2007) diffusion is the control mechanism for reduction of Fe_3O_4 in temperatures higher than 650°C. The next step was to investigate the behavior of the functions on the Arrhenius curves, as can be seems in Figure 2. In addition, the activation energy (Ea) was obtained in each step.

In Step 1 (550-650°C), the functions A3 and R2 presented a liner trend in the Arrhenius curve. The diffusion was not expected in this step, as was mentioned previously. Furthermore, the nucleation has been mentioned by several researchers at the initial stage of oxide reduction (Themelis and Gauvin, 1962; Hayes, 1979). The Ea in this step was 41.1 kJ/mol from A3 function.

Between 700-800°C, the functions A3 and D1 presented a linear trend to Arrhenius curves, which indicates a mixed control mechanism. The Ea of this step is 89.1 kJ/mol. The third step (850-950°C) was controlled by diffusion with an Ea of 130.9 kJ/mol. The diffusion is mentioned as the main mechanism by Pineau *et al.*, (2007).

3.3 Products characterization

At 700 °C, here was noted the formation of a crust around the pellet, as is shown in Figure 3a. In addition, the morphological aspect (Figure 3b) and the EDS spectrum (Figure 3c) suggest an non sintered structure, composed mainly of metallic iron. The formation of this crust impairs the gas diffusion into the pellets, which evidences that diffusion is the main mechanism above 700°C (Chang and De Jonghe, 1984).

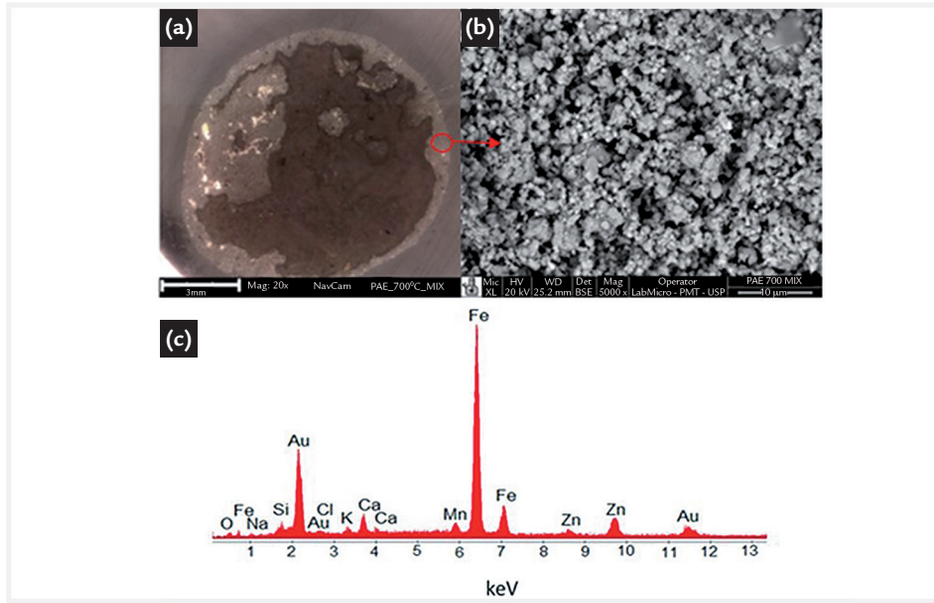

Figure 3
Images obtained for an electric arc furnace dust pellet at 700°C a) Image of optical microscope; b) Image of scanning electron microscope; c) EDS spectrum obtained in Figure 3b.

The metallic iron layer became thicker as the reaction proceeded. At 900°C, the reaction finished. The pellets presented a homogeneous aspect (Figure 4a) and sintered structure (Figure 4b) composed mainly of iron (Figure 4c). The formation of a sintered structure implies in a decrease of porous volume inside the pellet. Furthermore, the reduction reaction tends to be controlled via the internal diffusion of reducing gases (Hou, *et al.*, 2012).

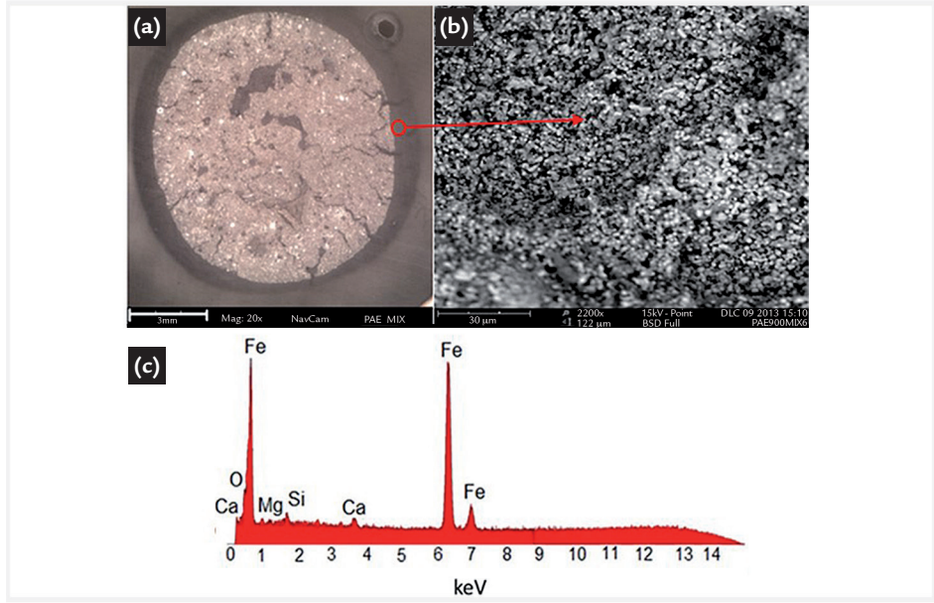

Figure 4
Images obtained of electric arc furnace dust pellet at 900°C a) Image of optical microscope; b) Image of scanning electron microscope; c) EDS spectrum obtained in Figure 4b.

In addition, Figure 5 shows the X-ray pattern obtained in the electric arc furnace dust pellet at 900°C.

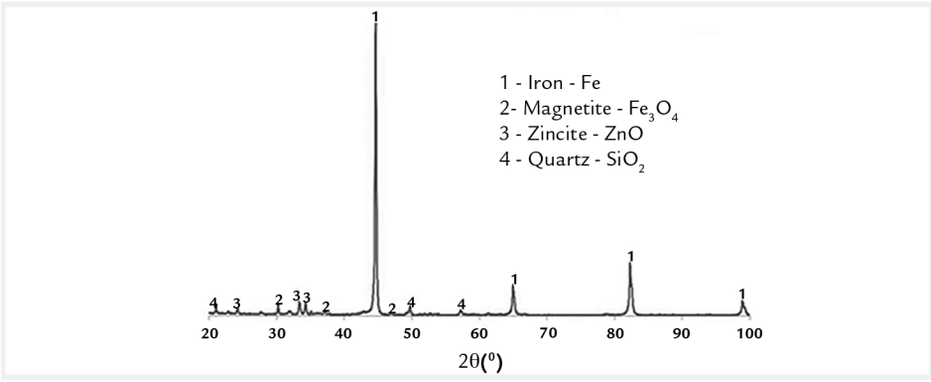

Figure 5
X-ray pattern obtained after complete reduction of the electric arc furnace dust pellet.

Peaks of iron, magnetite, zincite and quartz were noted. The phase's quantification by Rietveld method (Table 7) shows that the iron is the main phase with 82.8 wt%, while quartz, magnetite and zincite presented 11.0, 3.3 and 2.9 wt%, respectively. This indicates that the dense iron formed during the reaction prevented the complete reduction of the iron and zinc oxides.

Phases	Iron	Quartz	Zincite	Magnetite
Percentage (%)	82.8	11.0	2.9	3.3

Table 7
Quantification of phases from electric arc furnace dust pellets after complete reduction via Rietveld method.

4. Conclusion

A thermogravimetric test showed that the mass loss from the reduction of electric arc furnace dust using hydrogen was of 42 wt%, due to reduction of iron and zinc oxides. Furthermore, the reduction occurred in three steps: 550-650°C, 700-800°C, 850-950°C. The initial stage (550-650°C) was controlled by a nucleation mechanism with an Ea of 41.1 kJ/mol. For temperatures higher than 700°C an iron crust was formed around the pellet. This hindered the reducing gas diffusion into the pellet. Thus, in the second step (700-800°C), a mixed control between nucleation and diffusion was obtained with an Ea of 89.1 kJ/mol. In the temperature range of 850-950°C, the formation of a sintered structure was noted, which contributed to a decrease in the pore volume in the pellets. In addition, these facts indicated internal diffusion of reducing gases as the controlling mechanism. The Ea of this stage was 130.9 kJ/mol.

Acknowledgements

The authors would like to thank Universidade de São Paulo and Universidade do Extremo Sul Catarinense.

References

BROWN, M. E. Principles and Practice. ***Handbook of Thermal Analysis and Calorimetry.*** v.1, n.1, p. 691, 1998. ISBN: 978-0-444-82085-3.

CHANG, M., DE JONGHE, L. C. Whisker growth in reduction of oxides. ***Metallurgical Transactions B,*** v. 15B, p. 685-694, 1984.

CHEN, F., SORENSEN, O. T., MENG, G., PENG, D. Thermal decomposition of BaC2O4.0,5H2O studied by stepwise isothermal analysis and non-isothermal thermogravimetry. ***Journal of thermal analysis,*** v. 53, p.397-410, 1998.

HAYES, P. C. The kinetics of formation of H_2O and CO_2 during iron oxide reduction. ***Metallurgical Transactions B,*** v. 10B, p. 211-217, 1979.

HOU, B., ZHANG, H., LI, H., ZHU, Q. Study on kinetics of iron oxide reduction by hydrogen. ***Chinese Journal of Chemical Engineering,*** v. 20, p. 10-17, 2012.

JUNCA, E., ESPINOSA, D. C. R., TENÓRIO, J. A. S. Characterization of dust generated in electric arc furnace. In: INTERNATIONAL CONFERENCE SOLID WASTE TECHNOLOGY MANAGEMENT, 27. Philadelphia, 2012. p. 700-707.

JUNCA, E., RESTIVO, T. A. G., OLIVEIRA, J. R., ESPINOSA, D. C. R., TENÓRIO, J. A. S. Reduction of electric arc furnace dust pellets by simulated reformed natural gas. ***Journal of Thermal Analysis and Calorimetry,*** v. 126, p. 1889-1897, 2016.

KHAWAM, A., FLANAGAN, D. R. Solid-state kinetic models: basics and mathematical Fundamentals. ***Journal of Physical Chemistry B,*** v. 110, p. 17315-17328, 2006.

LEDESMA, E. F., JIMÉNEZ, J. R., AYUSO, J., FERNÁNDEZ, J. M., BRITO, J. Ex-

perimental study of the mechanical stabilization of electric arc furnace dust using fluid cement mortars. Journal of Hazardous Materials, v.326, p. 26–35, 2017.

LIN, Q., LIU, R., CHEN, N. Kinetics of direct reduction of chrome iron ore. ***Journal of Thermal Analysis and Calorimetry,*** v. 58, p.317-322, 1999.

MAQUEDA, L. A. P., ORTEGA, A., CRIADO, J. M. The use of master plots for discriminating the kinetic model of solid state reactions from a single constant-rate thermal analysis (CRTA) experiment. ***Thermochimica Acta,*** p. 165-173 and p. 277, 1996.

NEZHAD, S. M. M., ZABETT, A. Thermodynamic analysis of the carbothermic reduction of electric arc furnace dust in the presence of ferrosilicon. ***Calphad,*** v. 52, p. 143–151, 2016.

PINEAU, A., KANARI, N., GABALLAH, I. Kinetics of reduction of iron oxides by H2 Part II. Low temperature reduction of magnetite. ***Thermochimica Acta,*** v. 456, p.75–88, 2007.

SAYADI, M., HESAMI, S. Performance evaluation of using electric arc furnace dust in asphalt binder. ***Journal Clean Production,*** v. 143, p. 1260-1267, 2017.

THEMELIS, N. J., GAUVIN, W. H. Mechanism of reduction of iron oxides. ***Canadian Mining and Metallurgical Bulletin,*** v.55, p. 444-456, 1962.

Received: 4 December 2017 – Accepted: 29 June 2018.